CORA Cork Open Research Archive
Cartlann Taighde Oscailte Chorcaí

Title	An XPS study of the oxidation of reduced ceria-lanthana nanocrystals
Authors	Fleming, Peter G.;Ramirez, S.;Holmes, Justin D.;Morris, Michael A.
Publication date	2011-04-30
Original Citation	Fleming, P., Ramirez, S., Holmes, J. D. and Morris, M. A. (2011) 'An XPS study of the oxidation of reduced ceria–lanthana nanocrystals', Chemical Physics Letters, 509(1), pp. 51-57. doi: 10.1016/j.cplett.2011.04.090
Type of publication	Article (peer-reviewed)
Link to publisher's version	http://www.sciencedirect.com/science/article/pii/S0009261411005343 - 10.1016/j.cplett.2011.04.090
Rights	© 2011 Elsevier Ltd. All rights reserved. This manuscript version is made available under the CC BY-NC-ND 4.0 licence. - https://creativecommons.org/licenses/by-nc-nd/4.0/
Download date	2026-11-03 14:32:57
Item downloaded from	https://hdl.handle.net/10468/9701



UCC
University College Cork, Ireland
Coláiste na hOllscoile Corcaigh

Accepted Manuscript



An XPS Study of the Oxidation of Reduced Ceria-Lanthana Nanocrystals

P. Fleming, S. Ramirez, J.D. Holmes, M.A. Morris

PII: S0009-2614(11)00534-3
DOI: 10.1016/j.cplett.2011.04.090
Reference: CPLETT 29259

To appear in: *Chemical Physics Letters*

Received Date: 2 March 2011
Accepted Date: 27 April 2011

Please cite this article as: P. Fleming, S. Ramirez, J.D. Holmes, M.A. Morris, An XPS Study of the Oxidation of Reduced Ceria-Lanthana Nanocrystals, *Chemical Physics Letters* (2011), doi: 10.1016/j.cplett.2011.04.090

This is a PDF file of an unedited manuscript that has been accepted for publication. As a service to our customers we are providing this early version of the manuscript. The manuscript will undergo copyediting, typesetting, and review of the resulting proof before it is published in its final form. Please note that during the production process errors may be discovered which could affect the content, and all legal disclaimers that apply to the journal pertain.

ACCEPTED MANUSCRIPT

An XPS Study of the Oxidation of Reduced Ceria-Lanthana Nanocrystals

P Fleming[1,2*], S Ramirez[3], J D Holmes[1,2,4,5] and M A Morris[1,2,4,5]

[1]Department of Chemistry, University College Cork, Cork, Ireland
[2]Environmental research Institute, University College Cork, Cork, Ireland
[3]Department of Chemistry, University College Dublin, Dublin, Ireland
[4]Tyndall National Institute, Lee Maltings, Cork, Ireland
[5]CRANN, Trinity College Dublin, Dublin, Ireland
* Corresponding author email – Peter.Fleming@UCC.ie
Tel - 00353214901965

Key Words: Ceria, lanthana, solid solutions, x-ray photoelectron spectroscopy, oxidation-reduction

Abstract

Detailed x-ray photoelectron spectroscopy (XPS) studies on the oxidation of an extensivley cleaned, reduced ceria-lanthana solid solution (12.5 mol% La to Ce) was performed. Uptake of oxygen during oxidation followed a logarithmic dependence on exposure. Differential charging during oxidation suggests that the oxidation process is diffusion limited. No evidence for surface 3+ cerium states in the fully oxidised samples, which are anion defect free within the limits of experimental accuracy, was found. The data suggest that there is no evidence for the inherent stability of anion vacancies (associated with Ce^{3+} sites) at the surface of these nanocrystals.

Introduction

Cerium dioxide, ceria, has been of the subject of considerable research interest because of its interesting defect (non-stoichiometry) chemistry and its use in a number of catalyst systems, notably the three way automotive catalyst [1]. It also finds uses as a polishing material [2], an ionic conductor in fuel cells [3] and in gas sensors [4]. It has been studied in depth using XPS because of unusual mixture of 'shake-up' and 'shake-down' satellites which are observed [5]. The redox chemistry of ceria, at the heart of most of its practical use, has been studied using XPS a number of times using single crystals [6,7], foils [8], films [9,10,5,11], powders [12,13]

ACCEPTED MANUSCRIPT

and supported materials [14]. These studies clearly show that ceria (CeO_2) can be readily reduced by Ar^+ ion bombardment, H_2 or CO treatments to ~Ce_2O_3 and is re-oxidised back to ~CeO_2 on exposure to oxygen as observed using peak shape and shifts of the Ce3d and other core-levels peaks. However, the complex final state effects seen in Ce XPS spectra (as first explained by Burroughs et al and whose explanation is normally followed by later authors [15]) make quantification of the Ce^{3+}/Ce^{4+} ratio and the stoichiometry difficult. The non-stoichiometry of ceria is relatively complex because the so-called Ce^{3+} ion in the oxide is actually a Ce^{4+} ion coupled to a small polaron state and two of these are associated with each anion vacancy [16,17]. There is disagreement on whether a kinetically or thermodynamically stable surface "Ce^{3+}" species can exist at these oxidised samples because of additional stability of these species at the surface compared to the bulk. However, theory suggests that the formation of significant numbers of surface anion vacancies is only possible in UHV conditions at elevated temperatures [18]. Absolute experimental verification of surface stoichiometry by XPS is probably not possible because of electron and x-ray induced reduction of ceria and cerium compounds [19-22].

Whilst ceria has been very extensively studied, it is highly appropriate to extend these studies to ceria loaded with other lanthanide oxides such as lanthanum oxide. Lanthana forms solid solutions with ceria of expected formula $Ce_{1-x}La_xO_{2-x/2}$ and is typical of many tri-valent lanthanide oxides which are added to improve ionic/electronic conductivity and catalytic activity [1]. The marked improvement in activity of ceria-lanthana solid solutions in catalysis was first demonstrated by Mackrodt et al for the combustion of methane [23]. Wilkes et al showed that the rate of combustion over loaded catalysts compared to pure ceria could be improved by as much as factors of 3 [24]. Bernal and co-workers suggest that the additional activity of these systems is a result of increased ease of reduction and also morphological stability [25]. Reddy et al report that doping can improve oxygen storage capacity compared to ceria by factors of 4-5 and lower light-off temperatures for CO oxidation by 58 K [26].

XPS studies of the redox of $Ce_{1-x}La_xO_{2-x/2}$ are somewhat scant compared to the ceria system. Trudeau and co-workers provide a reasonably detailed study but use CO_2

ACCEPTED MANUSCRIPT

as an oxidising gas which may lead to problems with carbonate production [27]. These authors also report that as-synthesised material consists of a mixture of Ce^{3+} and Ce^{4+} states (an observation supported by Reddy et al [26]) and is reduced by vacuum, exposure. Du et al report the effects of argon ion bombardment of both ceria and $Ce_{1-x}La_xO_{2-x/2}$ but no controlled oxidation of the sample is reported [28]. Because of the absence of any extensive study of the redox properties of $Ce_{1-x}La_xO_{2-x/2}$ using XPS and the importance of this material, we report a study of an Ar^+ reduced 12.5 mole% (La to Ce) solid solution of lanthana-ceria. The value of 12.5% Lanthana doping was chosen as in catalysis studies this level appears to produce optimum reactivity [1].

Experimental

Preparation: Samples were made by simple reverse precipitation by addition of a 2M mixed cerium-lanthanum nitrate solution (at the target Ce:La molar ratio) to a NH_4OH solution (in excess). In this work a 12.5 mole % La to Ce was principally studied although a 100% ceria sample and other ceria-lanthana solid solutions were also prepared for comparison. The reverse precipitation was used as it produces small crystallite (nanocrystals) bearing powders with a highly homogenous distribution of the cations. Solid was recovered by filtration, washed several times in water and dried overnight at 373 K. The material was subsequently calcined at 1273 K for 12 hours. As shown by us previously, it is absolutely imperative to heat at these temperatures to ensure removal of stable hydroxide and carbonate phases although it should be noted that bulk hydroxylation/carbonation can occur on extended exposure to ambient and thus samples were processed for analysis as quickly as possible after calcination [29].

Characterisation: The reactivity of lanthanide oxides in ambient is poorly appreciated and we suggest that this is part of the reason that researchers see inconsistent XPS data for 'as-prepared samples'. A 12.5% molar ratio of La to Ce was used for the XPS studies detailed herein. The powder samples were pressed into 0.5 mm discs at 20 tonne per cm^{-2} pressure for XPS studies. Following pressing the samples were re-calcined before mounting onto steel stubs for XPS measurements. Samples were heated in the sample chamber by placing stubs in a resistively heated shroud (maximum 1273 K). Samples could be exposed to oxygen to a pressure of around 5×10^{-5} mbar in the analysis chamber. The samples were carefully cleaned

ACCEPTED MANUSCRIPT

prior to analysis. This consisted of heating in UHV for 2 hours to a temperature of 1073 K to remove carbonate. The sample was transferred into an *insitu* high pressure cell and heated in O_2 at 0.5 atm at 573 K for 45 min. It was then heated in H_2 at the same pressure for a further 45 minutes. This was then repeated a further twice. The reduced sample was then heated in UHV to 1000 K for 15 minutes before exposure to 10^{-5} mbar O_2 for several hours to affect complete oxidation. XPS data on the sample indicated only La, Ce and O and no indication of C and other contamination could be observed. XPS data were collected on a Vacuum Science Workshop CLASS100 high performance hemispherical analyser using Al Ka exciting radiation. A pass energy of 50 eV was used to minimise analysis times and so avoid x-ray induced photoreduction and other effects. The background pressure in the analysis chamber was 2 x 10^{-10} mbar. The samples were subjected to room temperature argon ion (Ar^+) bombardment (10 kV, 2 mA for 30 min) to affect reduction. Samples were then heated for 1 h at 673 K to restore surface order and remove any possible adsorbed contamination. Data were analysed by the usual methods. Peak areas were measured after a Shirley background subtraction [30]. Curve-fitting was carried out using a Doniach-Sunjic peak shape [31]. Peak asymmetry and peak widths were fixed, their values determined by fitting data from fully reduced and fully oxidised materials. An electron flood gun for charge neutralisation proved ineffective because of differential charging related to oxidation and also it was seen to bring about significant surface reduction. For La 3d and Ce 3d data presented here no charge correction has been carried out. This was decided on for a number of reasons, firstly, the fully reduced samples appeared very conductive with binding energies similar to that expeceted for the material and secondly It was of interest to this study to graphically depict the effect of oxidation on the conductivity of the sample. The O 1s spectra for the reduced sample also showed no charging, however, once charging was apparent the spectra were fitted and the lattice O^{2-} peak was corrected to the same position observed for the reduced, conducting, sample (530.0 eV).

Samples were also characterised by powder x-ray diffraction (PXRD). PXRD patterns were recorded on a Phillips M-PRO diffractometer equipped with a PIXEL detector using CuKa radiation at a working voltage is 40 kV. 5% w/w of zirconia was added as an internal reference to the solid solutions so that reflection positions and hence

ACCEPTED MANUSCRIPT

lattice parameters could be accurately determined. Total external reflection x-ray fluorescence (TXRF) was used to confirm the metal cation ratio of the synthesised powder. Data were collected on a Bruker S2 PICOFOX TXRF instrument and quantification was via peak fitting combined with full matrix calculations combined with analysis of physical mixtures of CeO_2 and La_2O_3 to ensure accuracy.

Results

Routine analysis data are shown in figure 1. The preparation was very reproducible and the metal ion composition of several preparations was within 1% of target as shown by indicative TXRF data (figure 1(A)). PXRD data show the expected lattice expansion of La_2O_3-CeO_2 solutions compared to CeO_2. Figure 1(B) shows PXRD data for ceria and the 12.5% La_2O_3 loaded sample (12.5La-Ce). Reflections observed are typical for the fluorite structure (JCPDS file No. 04-0593). The (111) reflection from the fluorite-like lattice of zirconia can be clearly resolved for the ceria sample. The ceria samples show doublets for the reflections due to the resolution of the Cu $K_{1,2}$ x-ray lines. The reflections for the 12.5La-Ce sample are not as well resolved as those of CeO_2 suggesting that the materials have smaller crystallite size. The mean crystallite size as estimated by Scherrer analysis of peak widths was 145 nm. The measured particle size for the as synthesised powders was 15 nm. This increase in particle crystallite size can be attributed to sintering during calcination. The addition of lanthana and its' reduction of the sintering rate of ceria has been noted previously [24] and the effective decrease in crystallite size probably results from increased lattice strain which reduces ion mass transport. The lattice expansion indicated by changes in position of the (111) reflections (figure 1(C)) shows the reflection for the 12.5La-Ce sample at lower angles than ceria and this is consistent with the well known lattice expansion that results from incorporation of the larger La^{3+} cation [16]. The variation of lattice parameter versus loading is described in figure 1(D).

XPS data for the 12.5La-Ce sample after Ar^+ bombardment and subsequent oxidation by exposure to oxygen (from 0 to 10, 000 L) at room temperature are summarised in figures 2, 3 and 4. La 3d data are shown in figure 2 and show a complex peak envelope that changes in shape and position through the oxidation process. The Ar^+ reduced sample (figure 2(A)) shows no charging and La 3d peaks are at binding energies typical of La_2O_3 values previously reported [32]. La 3d

ACCEPTED MANUSCRIPT

spectra obtained up to an exposure of 250 L remained conductive with no obvious charging effects. For samples above this exposure a gradual increase in charging is apparent as the sample oxidises and becomes more insulating. The main features in the La 3d spectrum, figure 2, are marked T, T*, S and S*. These are the $3d_{5/2}$ (T) and $3d_{3/2}$ (T*) features with accompanying shake-up satellites due to O 2p to La 4f electron transfer in the photoelectron final state. A peak shoulder around 830 eV BE (binding energy) can just be seen in the spectra resulting from low oxygen exposures. This is a cerium MNN Auger peak [33]. The position of the La 3d quadruplet, below an exposure of 250L, shows that peak shifts are negligible within experimental accuracy. However, above this exposure, the data become progressively more complex until at the end of the exposure regime (10,000L) a quadruplet is again observed (together with the low binding energy feature associated with the Ce MNN Auger feature, see arrow in figure 2 (h)) but these are all shifted to higher binding energy. The shift between data at low and high exposures can be attributed to a charge shift of about 5.6 eV caused by the sample becoming more electrically insulating as it reaches its stoichiometric lanthanide to oxygen ratio. Between exposures of 250 L and 5000 L (figure 2(E) to figure 2(G)) additional features can be seen within highly complex peak envelopes. It is asserted that this is due to differential charging of the sample due to incomplete oxidation. Ce 3d angle resolved data (discussed further below) collected at 10° grazing emission from a sample after 1000 L exposure suggest that the surface is completely oxidised. It, therefore, appears that oxidation of the sample bulk is limited by oxygen mass transport from the surface to the interior of the nanocrystals. Similar shifts were seen in all XPS data.

Of course, the La 3d photoelectron features are largely insensitive to reduction since the La^{3+} cation is not likely to show any other valence in combination with oxygen nor is it likely to be reduced to the metal. The reduction and re-oxidation of the sample is most evident in the Ce 3d features which are sensitive to non-stoichiometry and oxidation state as discussed above. Typical data for the Ce 3d XPS features are shown in figure 3. Data after initial Ar^+ treatment (figure 3(a)) and after exposure to 10,000L of oxygen (figure 3(h)) show peak shapes typical of Ce^{3+} and Ce^{4+} respectively. The reduced material (figure 3(a)) principally shows a double doublet structure reminiscent of the La 3d XPS data described in figure 2 and the individual

ACCEPTED MANUSCRIPT

features are labelled S*, S, T and T* following this description. In this case however, the satellite peaks are shake down not shake up peaks which is a result of the lowering of 4f band below the Fermi level for Ce^{3+} in comparison to La^{3+} for which the 4f band is above the Fermi level. There is a weak feature at higher binding energy (u''') which derives from non-reduced ceria. This may derive from either oxidation via contamination during Ar^{+} treatment or, we suggest more likely, due to the inelastic mean free path of the photoejected electrons being greater than the depth of film over which reduction is affected. At high exposures (figure 3(h)), the photoelectron features are typical of CeO_2. The contributions to this complex peak envelope are indicated in figure 3(h) and labelled as u, u', u'', u''' and v, v', v'', v''' according to Burroughs et al [15] where u and v represent the two different spin orbit ($3d_{5/2}$ and $3d_{3/2}$) contributions and the different prime states correspond to different final states caused by differing magnitudes of charge transfer between the Ce 4f band and O 2p valence band. The u''' and v''' represent the $Ce4f^0$-$O2p^6$ final state, while u, v and u'', v'' can be assigned to the $Ce4f^2$-$O2p^4$ and $Ce4f^1$-$O2p^5$ contributions respectively. These are all indicative of the Ce^{4+} oxidation state (CeO_2). Peaks u_o, u' and v_o, v' deriving from the Ce^{3+} oxidation state (Ce_2O_3) correspond to final states of $Ce4f^2$-$O2p^5$ and $Ce4f^1$-$O2p^6$[6, 14]. The data for the most extensively oxidised sample (figure 3(h)) shows little visible signs of features u' and v' (and detailed curve fitting shows no contribution of these states) and consequently suggest that the sample represents and effectively completely re-oxidised material. Between these two extremes the Ce 3d spectra show a complex mix of these contributions further complicated by the differential charging originating from the variation in oxidation as a function of depth into the nanocrystals (as described above). This differential charging is clearly manifest in the u''' feature which shows a clear doublet at intermediate exposures (marked with arrows in figure 3). It should be noted that similar studies have been carried out on a pure CeO_2 foil [34]. While a similar oxidation rate was observed no differential charging was evident. Attempting to quantify the extent of re-oxidation by curve-fitting the data proved extremely difficult because of the presence of up to 16 individual features in the spectra. Although good fits could be obtained quantitative analysis was not possible because several peak combinations gave similar quality fits. Evidence for the progressive nature of the oxidation process from surface to bulk can be seen in figure 4. Here, data from the sample after 500 L oxygen exposure at normal (figure

ACCEPTED MANUSCRIPT

4a) and 10° (figure 4b) emission angles are shown. In the more surface sensitive direction (10° emission) there is no sign of any differential charging and the peak positions and shape are indicative of close to or fully oxidised material demonstrating that the surface is much more oxidised than the bulk and the bulk rather than the external surface contains the majority of the more conducting reduced Ce^{3+}.

The O1s data as a function of exposure are shown in figure 5. The samples show the same differential charging as seen in La 3d and Ce 3d spectra and this is most obviously manifested in figure 5(f) which shows an unusual doublet structure. The data has be charge corrected so the main O 1s intensity is centred around 530.0 eV typical of CeO_2, Ce_2O_3 and La_2O_3. Also visible in all the data is a shoulder at around 531.5 to 531.8 eV. It is better resolved at low exposures. This is because:- a) the electrical conductivity of the reduced materials results in better resolution, b) It is a proportionally larger contribution to the total O1s signal (as discussed in detail below) and c) is not deleteriously altered by the differential charging observed at higher exposures. The origin of these high binding energy O 1s features on ceria and other lanthanide materials has been ascribed to hydroxyl contamination [35], carbonate contamination [28], adsorbed oxygen species [13] and highly polarised oxygen anions close to a vacancy centre [10,11] . Since these samples were very carefully prepared by extensive cleaning and were subsequently heated after Ar^+ treatments prior to any measurements, it is difficult to rationalise the high binding energy feature to contamination or adsorbed oxygen. Since the sample changes from a state of almost entirely Ce^{3+} to Ce^{4+} through the oxidation cycle, it is hard to support the arguments made about the peak being anions associated with vacancy formation because one would expect the concentration of these high binding energy features to change dramatically through the oxidation process. This is not the case. Curve-fitting the O 1s data allows measurement of the ratio of the high binding energy feature (O_{high}) to the lower binding energy feature (i.e. O^{2-} at normal lattice positions (O_{latt})). The variation of the O_{high}/O_{latt} ratio versus exposure is shown in figure 6. Curve-fitting to two components results in a variation that shows a maximum ratio of around 0.44 at 500 L. However, because a doublet is formed (e.g. figure 5(f)) due to a charged and uncharged component in all XPS data, curve fitting at intermediate exposures to four peaks is necessary. The corrected curve

ACCEPTED MANUSCRIPT

shows an initial high value of 0.36 but after 5L of oxygen reaches a minimum value of around 0.26 through the whole exposure regime. The consistency of this value suggests that the O_{high} is not due to contamination or adsorbed species since it might be expected to increase with exposure. The constant value of the ratio with exposure is also evidence that the features are not associated with the anion vacancy contribution.

On this basis, it is suggested that the high binding energy O1s feature derives from an oxygen state associated with lanthanum ion inclusion since no variation with exposure is observed after initial exposure to oxygen. At low exposures a second contribution must be present and may result from additional surface defect states which are removed by the low oxygen exposure (at these low exposures they are unlikely to be sub-surface states). Without more data it is not possible to assign the high binding energy feature to a specific defect or surface species. However, it is noted that the thermodynamic stability of an oxygen (electron) hole (i.e. O^-) species being formed as a charge compensating defect (i.e. an alternative to the widely established vacancy formation mechanism) for La^{3+} inclusion into the ceria fluorite lattice has been recently proposed [36]. This would provide an elegant explanation of the observation of high binding energy O 1s features observed in this work.

The progression of oxidation can be measured from either the oxygen (O 1s) to metal (Ce 3d + La 3d) peak area ratio or from the ratio of Ce^{3+} to Ce^{4+} species estimated from the changing Ce 3d spectrum. The O 1s to (Ce 3d + La 3d) peak area ratio can be converted to atomic ratios using known photoejection cross-sections [37] and an instrument correction factor of 1.15 measured from a pure CeO_2 sample introduced and cleaned in the same way (as the 12.5La-Ce sample) and exposed to 50,000 L of oxygen. The same sample was used to measure the U'''/total Ce 3d peak area for a stoichiometric CeO_2 sample. Values are tabulated in table 1 and plotted as oxygen stoichiometry in figure 7. The values measured range from 1.55 to 2.01 from zero to 10,000 L O_2 exposure. The value of 1.55 measured after reduction is close to the expected value of 1.50 for a sample of stoichiometry Ln_2O_3 and the slightly higher value suggests incomplete reduction within the analyte area as noted in the description of the Ce 3d photoelectron data. The upper value of 2.01 measured is somewhat higher than expected because the stoichiometry of the sample should be $Ce_{1-x}La_xO_{2-x/2}$ or $Ce_{0.875}La_{0.125}O_{1.9375}$. Curve-

ACCEPTED MANUSCRIPT

fitting the Ce 3d data to estimate the Ce^{3+} contribution from the relative contribution of the u' and v' components was considered unreliable because of the differential charging in the spectra. Instead the ratio of the Ce 3d u''' satellite peak area to the total Ce 3d peak area was used together with the assumption that this is linearly dependent on the amount of Ce^{4+} present [8]. This assumption has been questioned but Romeo et al show little evidence for this assertion [14]. Values of the stoichiometry estimated from the u''' contribution are tabulated in table 1 and plotted in figure 7. In the table the measured U'''/total Ce 3d peak area ratio is referenced to the value obtained on the pure ceria sample as described above. The value of about 2 obtained from both methods suggests that the sample is essentially stoichiometric CeO_2 (within experimental accuracy) after an exposure of 10,000 L and there is no evidence for any Ce^{3+} states being present. The results of the two analysis methods are in reasonable agreement and the differences seen in slope may arise from non-linearity of u''' with oxygen content but in our opinion are probably reflective of slightly different depth sensitivity of the two methodologies. It can be seen in figure 7 that the oxygen stoichiometry is linearly dependent on the logarithm of the oxygen exposure. This form of uptake-exposure dependence is typical of a bulk oxidation limited by mass transport from the surface to the bulk [38] and is what might be expected from the arguments made above about oxidation resulting in depth related differential charging. As can be seen from the data described in figure 7 the sticking probability of oxygen at the surface is high whereby a 5 L exposure is sufficient to increase the stoichiometry from 1.55 to around 1.65.

Discussion

The incorporation of La^{3+} cations into the ceria fluorite lattice is expected to introduce anion vacancies ($V_{O,La}$) by means of charge compensation but they are not accompanied by any Ce^{3+} formation. By Ar^+ treatment we are further introducing an additional type of vacancy, V''_O, which are doubly positively charged relative to a normal lattice O^{2-} site with electrons being transferred to cerium cations (forming Ce^{3+} like states) via a small polaron. It is clear the Ar^+ treatment is an effective means of surface reduction with all but around 15% of the solid solution of the material being reduced to a composition of Ln_2O_3 within the surface and selvedge region. It is suggested the depth of this reduced volume is

ACCEPTED MANUSCRIPT

somewhat less than that defined by the Ce 3d photoelectron mean free paths. It may be argued that the 15% that is not reduced may result from contamination during argon ion treatment but this is considered unlikely as background pressures were maintained at low values.

Re-oxidation is rapid following Ar^+ reduction. After an exposure of 25 L the stoichiometry is around $LnO_{1.75}$ or about half the V''_O vacancies (in both the surface and interior of the sample) have been filled. With this rapid re-oxidation, which is clearly a surface process, it is difficult to consider any surface anion vacancies of the V''_O type remaining after oxidation is complete. This assertion is supported by angle resolved Ce 3d data. The kinetics of oxygen uptake are very suggestive that the process is mass transport (from surface to bulk) limited. The evidence presented here, thus, contradicts assertions by many authors that stable anion vacancy-Ce^{3+} defects can exist in ambient conditions at the surface of nanoparticles [39]. In direct conflict with our findings, authors have suggested that some anion defect structures can exist at the surface of oxidised ceria films based on angle resolved XPS studies [9]. Other authors have used a variety of surface techniques including XPS, XAS and EELS in a very detailed study to show that no such surface defects can exist [6]. Any differences in findings may simply be related to the possibility of surface reduction under x-ray or electron irradiation. Further, angle-resolved studies may be complex because the reduction depth can be less than the photoelectron escape depth.

Finally, some comment on the presence of the high binding energy O 1s feature should be made. Almost all authors working on ceria or Ln^{3+}-CeO_2 solid solutions have noted this feature. Here, we have shown that the peak observed here must be related to some sort of defect associated with La^{3+} insertion into the lattice. This may be either a form of oxygen (created by charge compensation of the lower valence lanthanum cations) such as O^- or from chemically shifted oxygen states because of association with a $V_{O,La}$ site. While we favour a defect related explanation rather than a binding energy shift caused by chemical shifts (since the relative amount of these chemically shifted species showed little dependence on the number of anion vacancies present) we acknowledge that the investigation of these is made difficult by the reactivity of these reduced surfaces and also problems

ACCEPTED MANUSCRIPT

in charge referencing [6]. This makes a categoric explanation difficult. It is clearly a subject that requires more extensive study in order to fully understand the origin of this peak.

Acknowledgements

This work was supported through the Science Foundation Ireland BioNanoInteract Strategic research Cluster Grant (07/SRC/B1155). SFI is also acknowledged through the Overhead Investment Plan which supported both instrument purchase and funding for P. Fleming.

References

[1] 'Catalysis by ceria and related materials', edited by Alessandro Trovarelli, Catalytic Series Vol II, World Scientific Books, New Jersey, US, 2002

[2] Shchukin D G, Caruso R A. Chem Mat 2004; 16:2287–92

[3] Jacobs G, Williams L, Graham U, Sparks D, Davis BH. J Phys Chem B 2003; 107: 10398–404

[4] Jasinski P, Suzuki T, Anderson HU. Sens Act B 2003; 95:73–7.

[5] Bagus P S, Nelin C J, Ilton E S, Baron M, Abbott H, Primorac E, Kuhlenbeck H, Shaikhutdinov S, Freund H –J. Chem Phys Letts 2010; 487:237–240

[6] Mullins D R, Overbury S H, Huntley D R. Surf Sci 1998; 409:307-319

[7] Henderson M A, Perkins C L, Englehard M H, Thevuthasan S, Peden C H F. Surf Sci 2003; 526: 1-18

[8] Creaser D A, Harrison P G, Morris M A, Wolfindale B A. Catalysis Letts 1994; 23: 13-24

[9] Juel M, Martinsen S, Raan S. Thin Solid Films 2008; 517: 805-810

[10] Škoda M, Cabala M, Matolínová I, Skála T, Veltruská K, Matolín V. Vacuum 2010; 84: 8-12

[11] Holgado J P, Munuera G, Espinós J P, González-Elipe A R. Applied Surf Sci 2000; 158: 164-171

[12] Holgado J P, Alvarez R, Munuera G. Applied Surf Sci 2000; 161: 301-315

[13] Wang G, Mu Q, Wang Y. J Alloys and Compounds 2010; 493: 2010-207

[14] Roméo M, Bak K, El Fallah J, Le Normand F, Hilaire L. Surf and Interface Analysis 1993; 20: 508-512

ACCEPTED MANUSCRIPT

[15] Burroughs P, Hamnett A, Orchard F and Thornton G. J C S Dalton 1976; 1686-1698

[16] Morris B C, Flavell W R, Mackrodt W C and Morris M A. J Mat Chem 1993; (1993), 3: 1007- 1013

[17] O'Neill W M, Morris M A. Chem Phys Letts 1999; 305: 389-394

[18] Fronzi M, Soon A, Delley B, Traversa E, Stampfi C. J Chem. Phys 2009; 132: 104701, 1-16

[19] Rama Rao M V, Shripathi T. J Electron Spectroscopy and Related Phenomena 1997; 87: 121-126

[20] El Fallah J, Hilaire L, Roméo M, Le Normand F, J Electron Spectroscopy and Related Phenomena 1995; 73: 89-103

[21] Zhang F, Wang P, Koberstein J, Khalid S, Chan S-W. Surf Sci 2004; 563: 74-82

[22] Sucorski Y, Gottfriedsen J, Wrobel R, Strzelczyk, Weiss H. Solid State Phenomena 2007; 128: 115-120

[23] Mackrodt W C, Fowles M, Morris M A. US Patent, 4,940,685

[24] Wilkes M F, Hayden P and Battacharya A K. J Catalysis 2003; 219: 286-294

[25] Bernal S, Blanco G, Cifredo G, Pérez-Omil, Pintada J M, Rodríguez-Izquierdo J M. J Alloys and Compounds 1997; 250: 449-454

[26] Reddy B M, Katta L, Thrimurthulu G. Chem Mater 2010; 22: 467-475

[27] Trudeau M L, Tschöpe A, Ying J Y. Surf And Interface Analysis 1995; 23: 219-226

[28] Du X-y, Li W-c, Liu Z-x, Xie K. Chin Phys Lett 1999; 5: 376-377

[29] Fleming P, Farrell R A, Holmes J D, Morris M A. J Am Ceram Soc 2010

[30] Shirley D A. Phys Rev B 1972; 5: 4709-4714

[31] Doniach S, Sunjic M. J Phys 1970; C3: 285–291

[32] Howng W-Y, Thorn R J. J Phys Chem Solids 1980; 41: 75-81

[33] Nelson A E, Schulz K E. Surf Sci Spectra 2000; 7: 281-296

[34] Creaser D A, Harrison P G, Morris M A, Woldindale B A. Catalysis letters 1994; 23: 13-24

[35] Pfau A, Schierbaum K D. Surf Sci 1994; 321: 71-80

[36] Yeriskin I, Nolan M. J Phys: Condens Matt 2010; 22: 135004

[37] Seah M P, Gilmore I S, Spencer S J. Surf Interface Anal 2001; 31: 778-795

[38] Veena Kumari S, Vaidyan V K, Sathyanarayana K G. J Mater Sci Lett 1990; 9: 1441-1442

[39] Tsunekawa S, Ito S, Kawazoe Y. Appl Phys Lett 2004; 85: 3845-3847

ACCEPTED MANUSCRIPT

Table 1: Estimated oxygen stoichiometry (see text for details)

Exposure, L	0	2.5	5	10	15	25	50	100	250	500	10^3	1.5×10^3	2.5×10^3	5×10^3	1×10^4
O1s/(La3d + Ce3d) peak area ratio	0.129	0.133	0.137	0.141	0.142	0.145	0.149	0.152	0.155	0.158	0.163	0.165	0.167	0.167	0.167
O/Ln ratio	1.55	1.60	1.65	1.70	1.71	1.75	1.79	1.83	1.86	1.90	1.96	1.98	2.01	2.01	2.01
U'''/Ce3d peak area ratio	0.17	0.22	0.28	0.40	0.41	0.44	0.53	0.55	0.60	0.70	0.75	0.79	0.83	0.95	1.00
O/Ln ratio	1.59	1.61	1.64	1.70	1.71	1.72	1.76	1.78	1.80	1.85	1.87	1.90	1.91	1.97	2.00

Note that the U'''/Ce3d peak area ratio is a relative value to the ratio obtained after an exposure of a cleaned 50,000 L. It is then assumed that this is equivalent to CeO_2.

Figure captions

Figure 1. Characterisation of samples by XRD and TXRF. (A) Typical TXRF data for 12.5 mole% La to Ce sample showing line positions. (B) and (C) XRD data for samples as wide scan and narrow scan respectively. In each case the bottom diffractogram is a ceria-only material for comparison whilst upper trace is the 12.5La-Ce sample. (D) Data summarising lattice expansion as a function of La^{3+} content.

Figure 2. Selected data showing La 3d photoelectron features from an Ar^+ reduced sample (a) and during re-oxidation. Data shown after 2.5 (b), 10 (c), 25 (d), 250 (e), 1000 (f), 5000 (g) and 10,000 L (h). Solid lines indicate the charge shift resulting from oxidation and the arrow (upper right) the Ce Auger feature.

Figure 3. Selected Ce3d XPS photoelectron data from an Ar^+ reduced sample (a) and during re-oxidation. Data shown after 2.5 (b), 10 (c), 25 (d), 250 (e), 1000 (f), 5000 (g) and 10,000 L (h). Peak assignments described in the text. The arrow shows the differential charged feature which is most obvious the u''' feature.

ACCEPTED MANUSCRIPT

Figure 4. Ce3d XPS data following 500L oxygen exposure at (a) normal and (b) 10 degrees grazing emission.

Figure 5. Selected O1s XPS photoelectron data from an Ar^+ reduced sample (a) and during re-oxidation. Data shown after 2.5 (b), 10 (c), 25 (d), 250 (e), 1000 (f), 5000 (g) and 10,000 L (h). Data have been charge corrected where appropriate.

Figure 6. O_{high} to O_{latt} peak area ratio as function of exposure. The dotted line shows the minimum value. Closed circles show curve-fitting to two peaks and open circles to four peaks (charged and uncharged contributions).

Figure 7. Oxygen-metal stoichiometry (as x in LnO_x) versus exposure. Closed squares are values derived from the O1s to Ce3d plus La3d peak area ratio and closed triangles from the Ce^{3+} to Ce^{4+} ratio from the Ce3d spectrum.

ACCEPTED MANUSCRIPT

Figure 1

ACCEPTED MANUSCRIPT

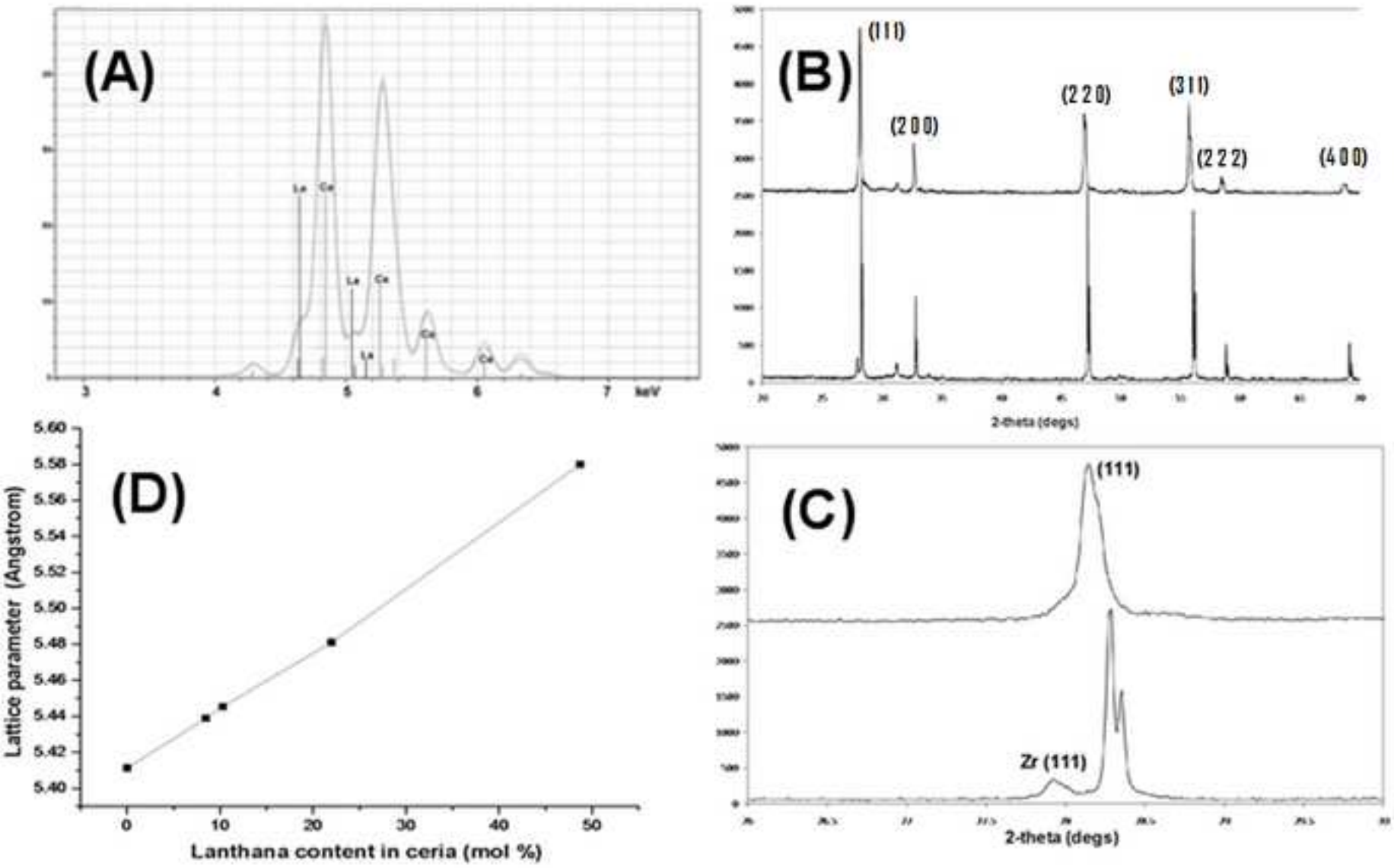


Figure 2

ACCEPTED MANUSCRIPT

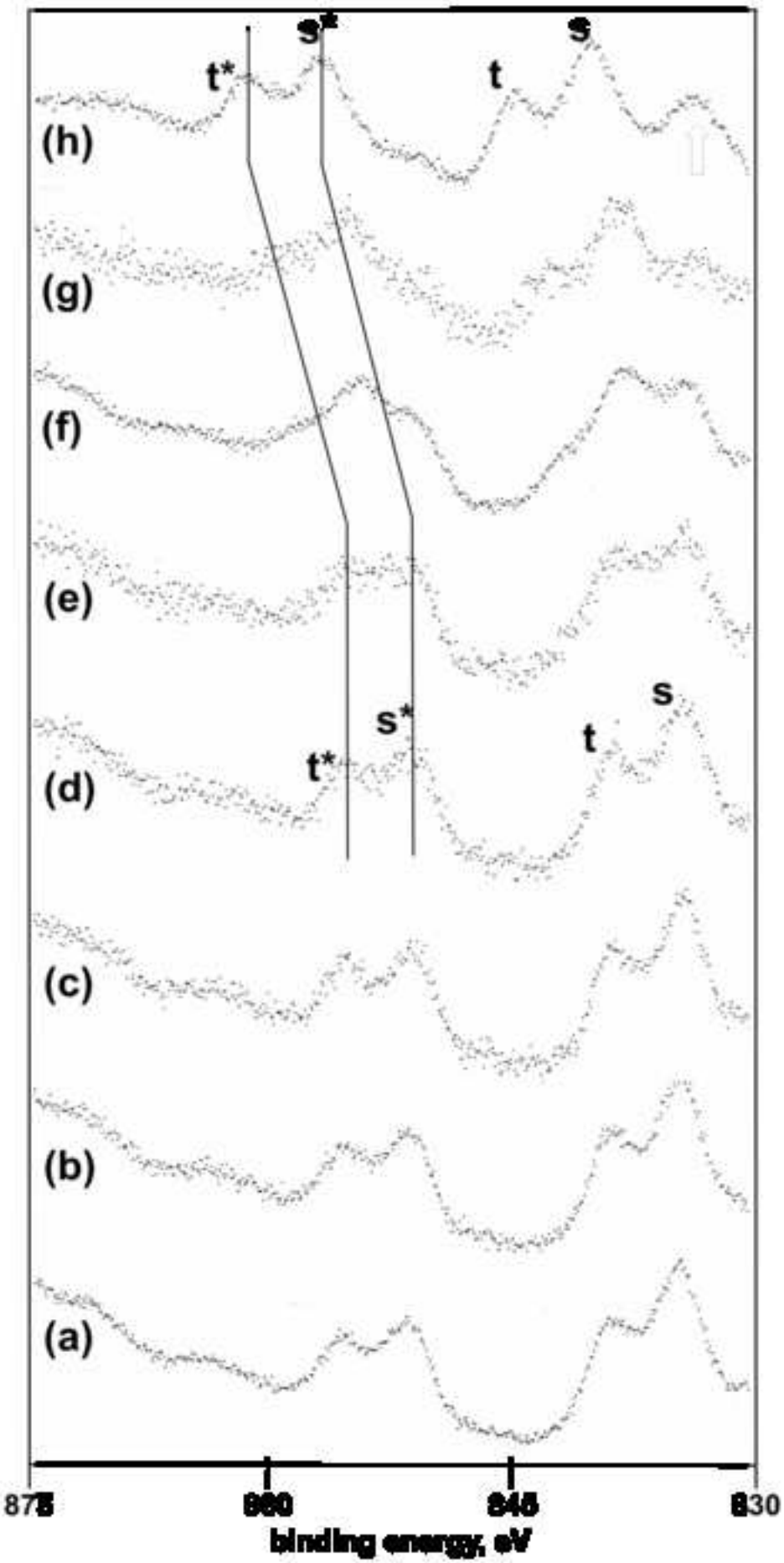


Figure 3

ACCEPTED MANUSCRIPT

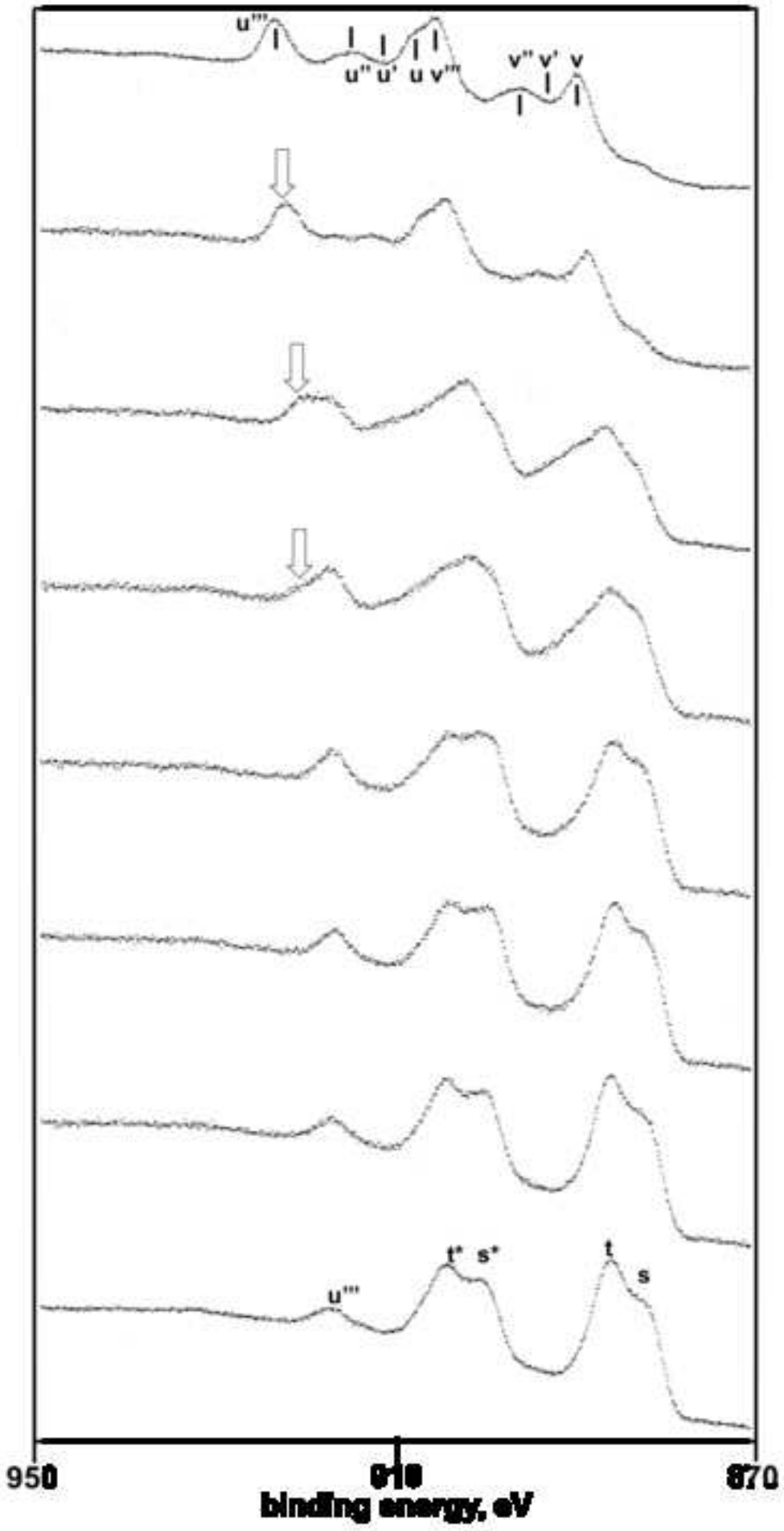


Figure 4

ACCEPTED MANUSCRIPT

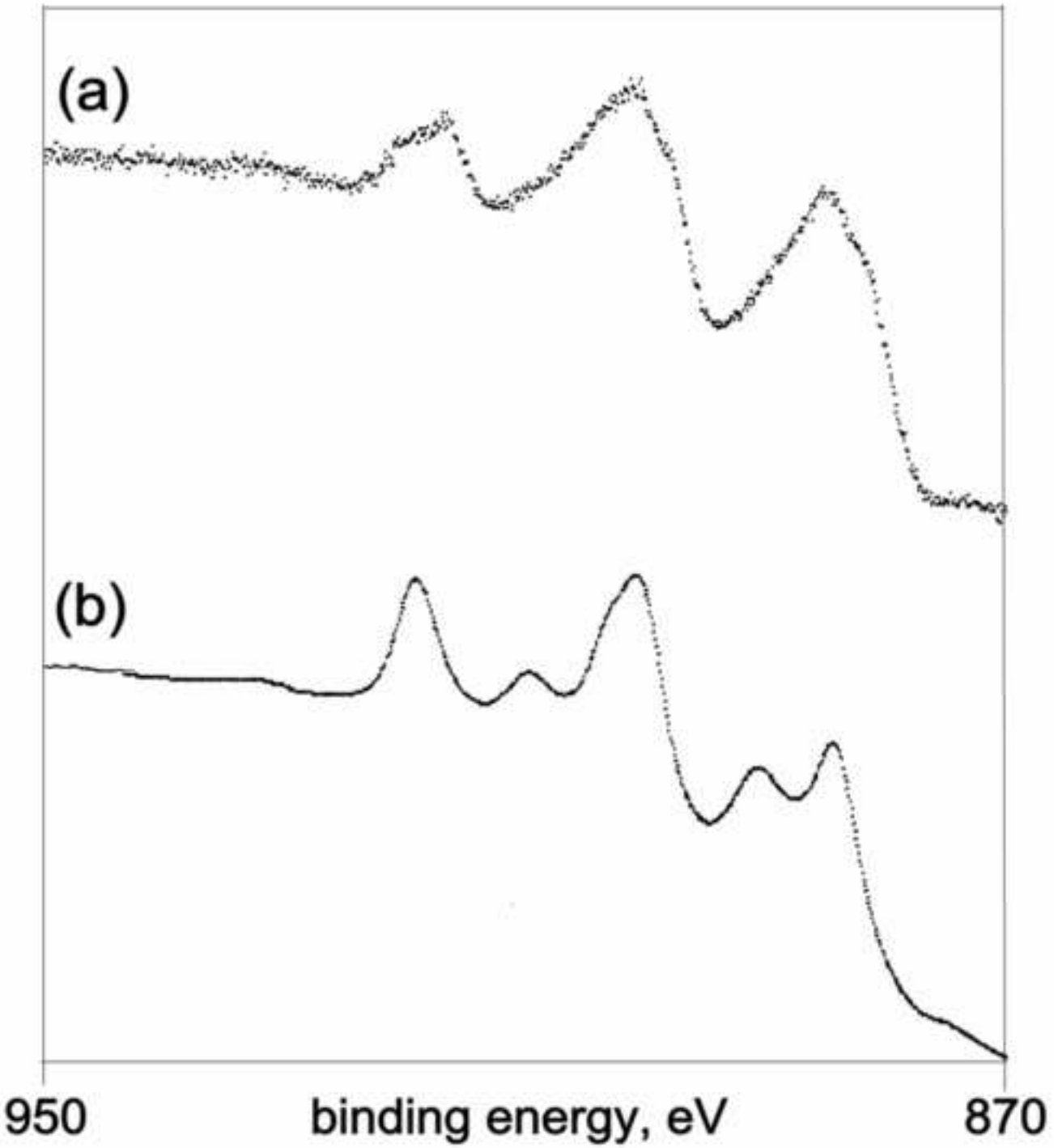


Figure 5

ACCEPTED MANUSCRIPT

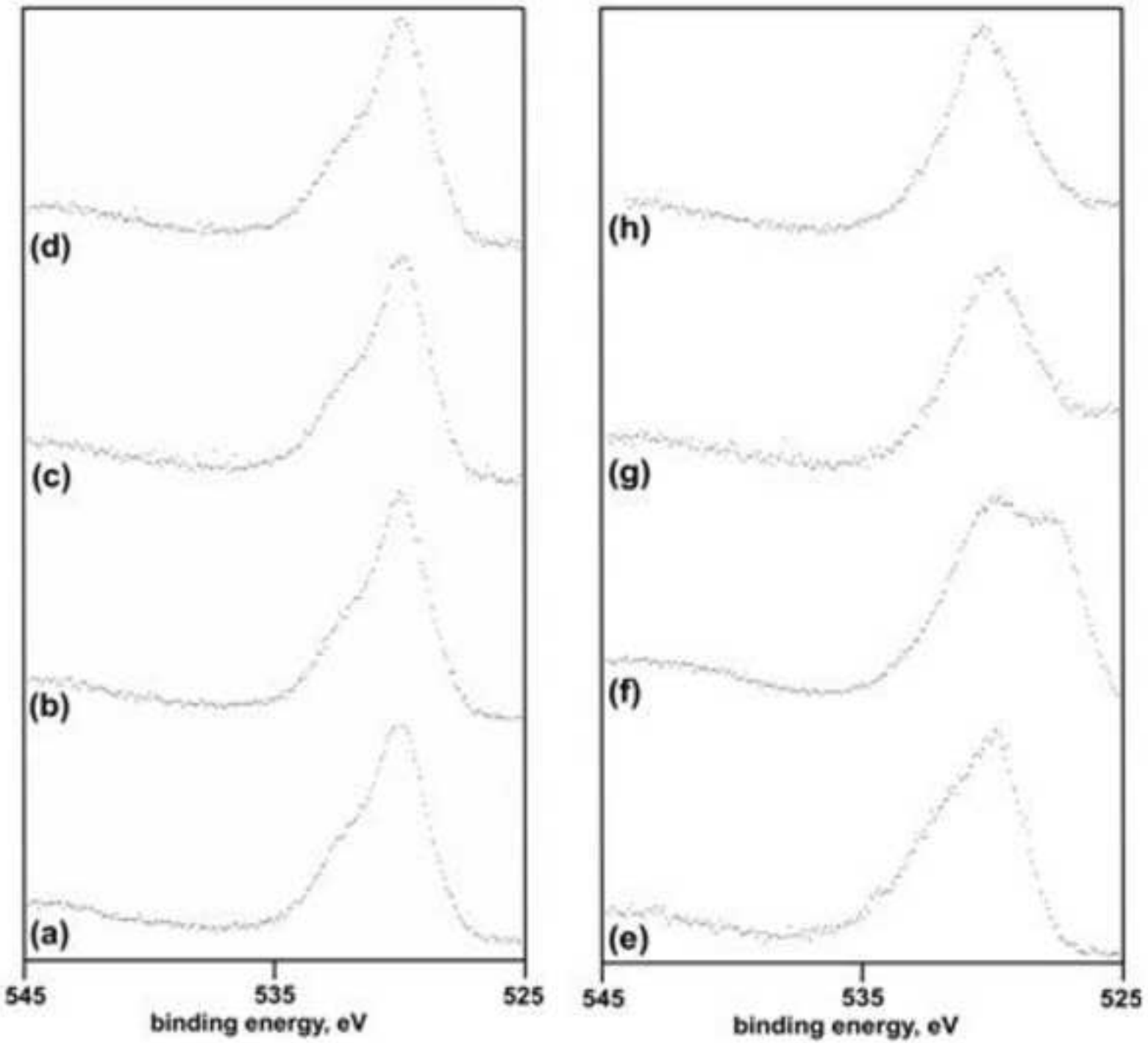


Figure 6

ACCEPTED MANUSCRIPT

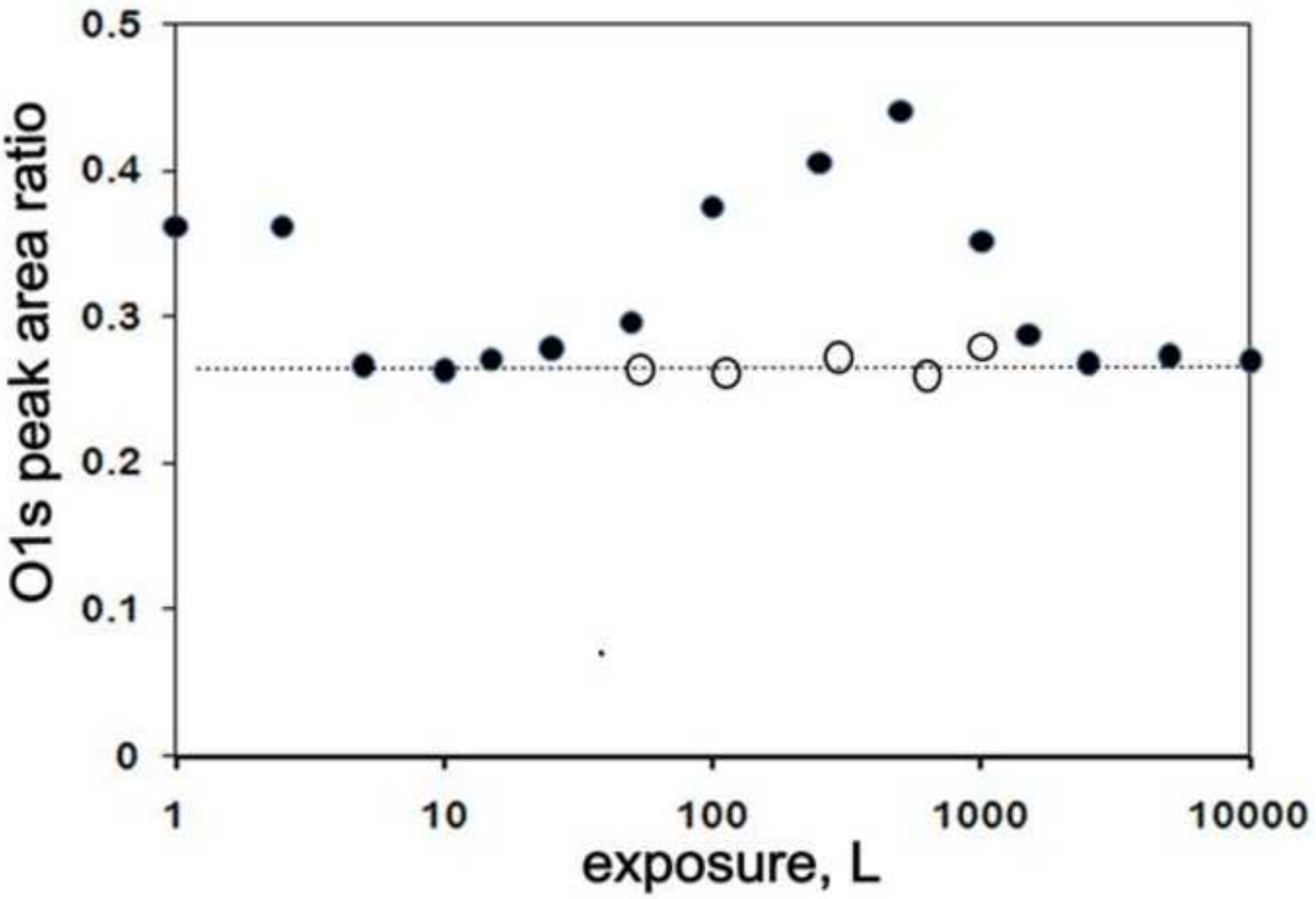
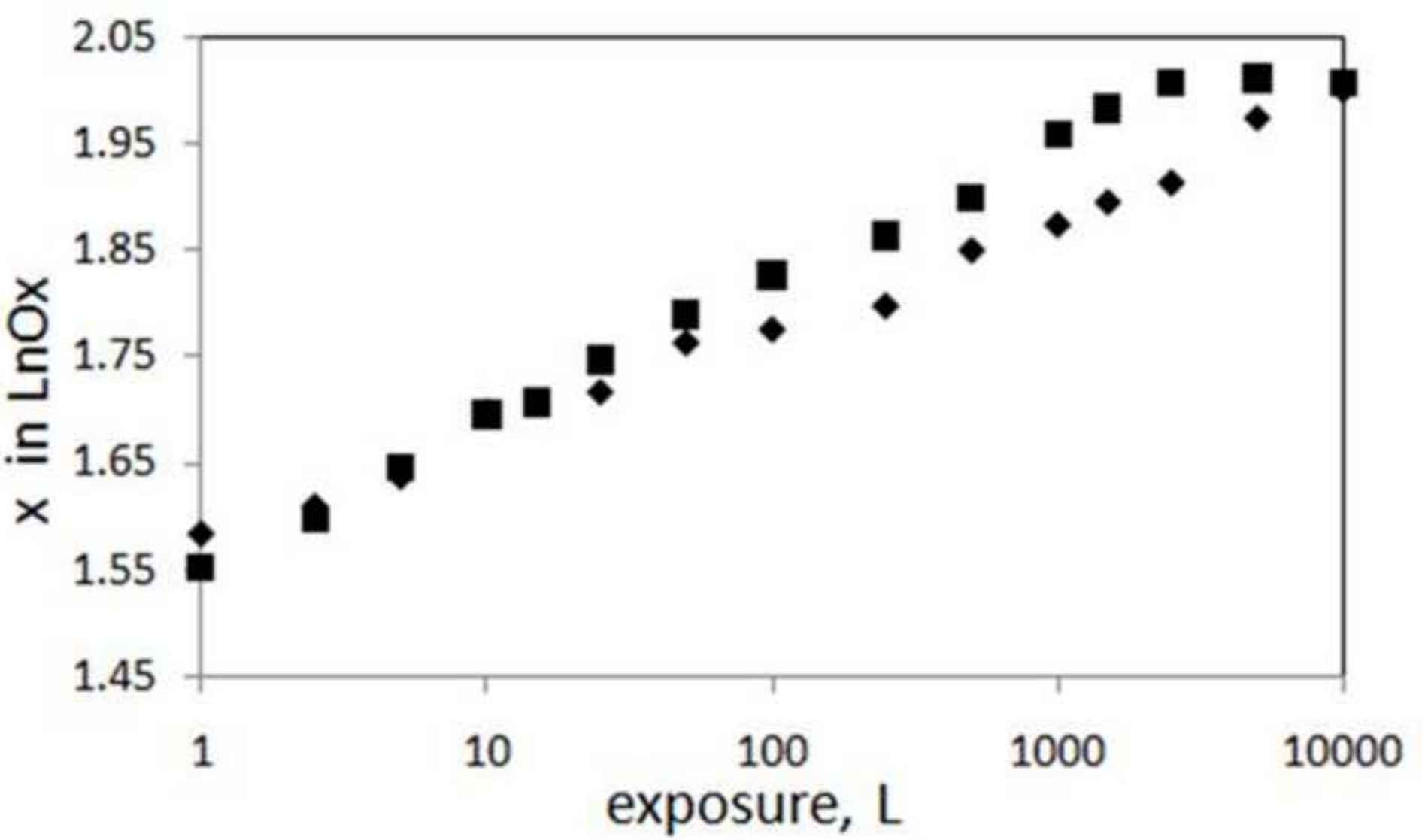


Figure 7

ACCEPTED MANUSCRIPT



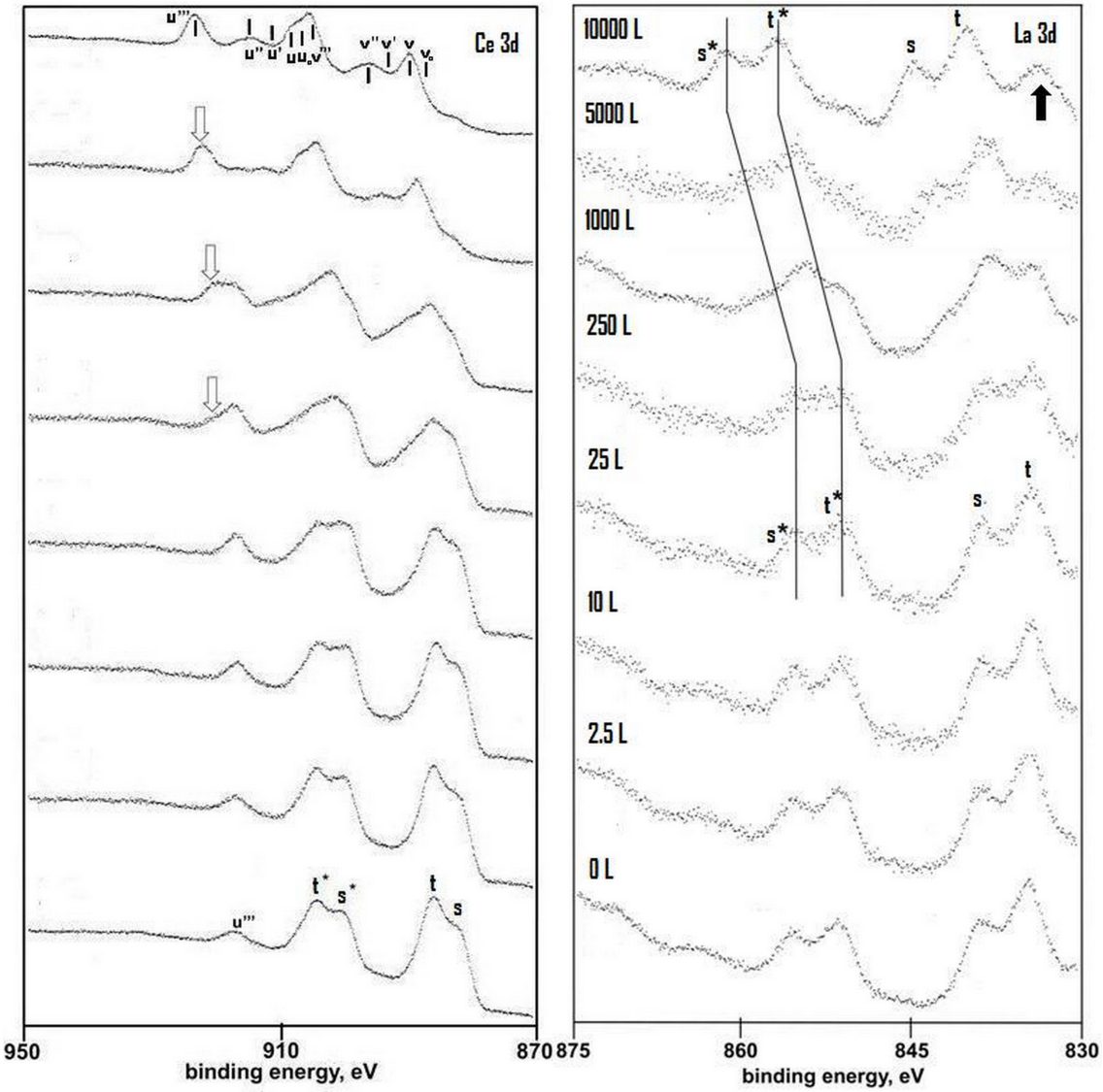
ACCEPTED MANUSCRIPT

1

2

3 Graphical abstract

4



5

6

ACCEPTED MANUSCRIPT

Below are the research highlights from our work entitled "An XPS Study of the Oxidation of Reduced Ceria-Lanthana Nanocrystals".

1. Oxidation was found to follow a logarithmic uptake.
2. Oxidation was found to be mass transport limited.
3. Ce^{3+} surface species found not to be stable under ambient conditions.
4. Lateral O1s peak found to be independent of V_o and Ce^{3+} concentration.

ACCEPTED MANUSCRIPT